

Brief Communication

The discovery of promising candidate biomarkers in kidney renal clear cell carcinoma: evidence from the in-depth analysis of high-throughput data

Xue Li*, Mingfeng Li*, Tianyu Zhao, Jingyu Zhang

Central People's Hospital of Zhanjiang, Zhanjiang, Guangdong, China. *Equal contributors.

Received May 4, 2023; Accepted July 11, 2023; Epub September 15, 2023; Published September 30, 2023

Abstract: Kidney renal clear cell carcinoma (KIRC) is the most prevalent subtype of renal tumor. The underlying mechanisms governing KIRC initiation and progression are less known. The present study aimed to reveal novel hub genes associated with the initiation and progression of KIRC, which may be utilized as novel molecular biomarkers and therapeutic targets for the treatment of KIRC. The GSE6344 dataset from the Gene Expression Omnibus (GEO) database was integrated to identify differentially expressed genes (DEGs) using the limma package. Then, hub genes were identified and UALCAN, GEPIA, OncoDB, DriverDBv3, GENT2, and HPA databases were employed for the expression, survival, and methylation analyses. cBioPortal tool was used to investigate the genetic alterations, while CancerSEA, TIMER, DAVID, ENCORI, DrugBank, and GSCAlite were utilized to explore a few more hub gene-associated parameters. Finally, targeted bisulfite sequencing (bisulfite-seq), and RT-qPCR techniques were used to validate the expression and methylation level of the hub genes using Human RCC cell line 786-O, A-498, and normal renal tubular epithelial cell line HK-2. In total, 7299 DEGs were found between KIRC and normal samples in the GSE6344 dataset. Using STRING and Cytohubba analysis, four hub genes including VEGFA (vascular endothelial growth factor), ALB (Albumin), ENO2 (enolase 2), and CAV1 (Caveolin 1) were selected as the hub genes. Further, it was validated through extensive analysis of TCGA datasets that these VEGFA, ENO2, and CAV1 hub genes were significantly up-regulated, while ALB was significantly down-regulated in KIRC samples compared to controls. The dysregulation of these genes was found to be associated with the overall survival (OS) of the KIRC patients. Moreover, this study also revealed some novel links between VEGFA, ALB, ENO2, and CAV1 expression and genetic alterations, promoter methylation status, immune cell infiltration, miRNAs, gene enrichment terms, and various chemotherapeutic drugs. The present study revealed a panel of four hub genes, which contributed to improving our understanding of the underlying molecular mechanisms of KIRC development and can be utilized as promising novel biomarkers for KIRC diagnosis, prognosis, and treatment.

Keywords: KIRC biomarker, expression analysis, prognosis

Introduction

Renal cell carcinoma (RCC) is one of the top ten malignant tumors in both males and females worldwide, accounting for more than 90% of pelvic malignancies and primary renal neoplasms [1]. Over the last few decades, the mortality rate due to RCC has risen considerably around the globe [2-4]. Kidney renal clear cell carcinoma (KIRC) is the most prevalent subtype of RCC, which accounts for more than 75% of cases and represents the most malignant genitourinary cancers [5]. Around one-fourth of KIRC patients were diagnosed at the late stage

with distal metastasis or advanced regional disease state [6].

Up till now, some major breakthroughs have been made in understanding the molecular mechanisms and identifying novel therapeutic targets in KIRC patients, but the overall survival (OS) of the KIRC patients is still very low (5-year survival <32%), specifically in those patients who have distal metastasis [7, 8].

Therefore, the exploration of reliable novel molecular biomarkers is urgently required to assist clinicians and researchers in understanding KIRC initiation at the molecular level and

promote its timely detection and treatment. Previously, it was observed that Polybromo-1 is the important factor for accelerating cell proliferation and metastasis across KIRC cells by dysregulating numerous metabolic pathways, such as the phosphatidylinositol 3-kinase (PI3K) pathway, the glucose uptake pathway, and different hypoxia response genes [9, 10]. The two clinically used diagnostic biomarkers of KIRC include carbonic anhydrase IX and vascular endothelial-derived growth factor [11]. However, the success rate of these biomarkers is still low [12, 13].

Over the last decade, advances in microarray and RNA-sequencing (RNA-seq) technologies, as well as the integration of bioinformatics tools with these technologies, have made it feasible for the researcher and clinicians to discover important diagnostic and prognostic biomarkers involved in cancer development, progression, and metastasis [14-17].

In the present study, we explored the GSE6344 [18] microarray dataset from the Gene Expression Omnibus (GEO) database to get differentially expressed genes (DEGs) among the KIRC patients group and normal individuals group, in order to determine hub genes as the reliable novel biomarkers associated with KIRC diagnosis and poor prognosis. Meanwhile, we used KIRC TCGA datasets to evaluate the utility and efficacy of the discovered hub genes as new biomarkers. Moreover, based on a gene-drug interaction network, this study also revealed a few potential drugs, that can reverse the gene expression of identified hub genes in KIRC patients, aiming for successful treatment. This study has uncovered and validated four potential biomarkers, including VEGFA (vascular endothelial growth factor), ALB (Albumin), ENO2 (enolase 2), and CAV1 (Caveolin 1), which are of great importance in diagnosis prognosis, and treatment of the KIRC patients. In a nutshell, the outcomes of the present study may contribute significantly to understanding the molecular pathways of KIRC development, progression, and metastasis.

Methodology

Data collection and preprocessing

The GEO database was thoroughly searched using the keywords “Kidney renal clear cell car-

cinoma” and “Kidney neoplasm”. The criteria utilized for selecting an appropriate KIRC dataset were as follows: (i) studies employing any form of pharmacological manipulation were excluded; (ii) studies utilizing interfering molecules such as miRNAs, siRNAs, or gene therapies of any kind were excluded; (iii) datasets involving knockdown cultures or artificially induced mutations were eliminated; (iv) studies with a minimum of fifteen control and fifteen experimental samples were selected; (v) studies exclusively performed in Homo sapiens were chosen; (vi) studies using xenograft techniques were removed; (vii) studies providing a clear description of the protocol or samples employed, with correct labeling, were selected; (viii) datasets that made their raw data available were chosen, excluding those that only provided the author’s treated data; (ix) studies performed on platforms not belonging to Affymetrix, Illumina, or Agilent manufacturers were excluded; and (x) samples from metastasized tissues were excluded. Ultimately, all studies until the end of 2022 were individually examined and manually curated. A total of 3 microarray datasets (including both single and dual channel experiments) were appeared. Based on enough sample size, the GSE6344 [18] dataset, containing 20 normal samples and 20 KIRC patient samples, was chosen as the experimental dataset. Additionally, we screened gene probes in the GSE6344 dataset before analysis. The expression data for all gene probes that lacked matching genes in the dataset was eliminated. Moreover, the average expression of all the probes for a gene with two or more probes was kept.

Identification of DEGs

The R language “Limma” package was used to find the DEGs in the KIRC and control sample groups. To evaluate the DEGs, the following selection criteria were used: $|\log_2FC|$ more than 0.3 and p (T-test, Empirical Bayes techniques) less than 0.05 [19, 20]. The Fold Change (FC) in expression highlights the considerable differences among DEGs.

Construction of PPI, module identification, and the selection of hub genes

For further investigation, in total 250 genes with the greatest expression differences in terms of p -values were chosen. With the use of

KIRC biomarkers

the STRNG database [21], the PPI of the selected 250 genes was created. In order to identify the critical module, the built PPI was submitted to MCODE analysis [22] using the Cytoscape tool [23]. The critical module was then screened through the Cytohubba function [24] in the Cytoscape tool to select the hub genes. Based on the 4 different scoring algorithms, the maximum neighborhood component (MNC), the density of the maximum neighborhood component (DMNC), the maximal clique centrality (MCC), and the Degree of the Cytohubba [25], the shared top four genes by these 4 algorithms were selected as hub genes.

UALCAN database

The Cancer Genome Atlas (TCGA) expression data is used to create gene expression plots based on various pathological factors in the UALCAN database, a new online web-based tool that enables users to perform interactive and customizable analyses between normal-v-normal cancer samples [26]. These analyses include differential gene expression profiling, correlation analysis, survival analysis, and gene expression plots based on different pathological stages. In our investigation, we used this database to confirm hub gene expression at the mRNA and protein levels in KIRC and normal samples. The *p*-value cutoff was selected as 0.05.

GEPIA, DriverDBv2, OncoDB and GENT2 databases

Then, to further validate hub genes' expression across KIRC tissues and cell lines, we employed the GEPIA [27], OncoDB [28], DriverDBv3 [29], and GENT2 [30] databases. All these online databases are cancer microarray-based expression analysis platforms, which provide expression analysis results in the form of box plots. Moreover, we also used GEPIA for the survival analysis of the hub genes. For expression and survival analyses between normal and KIRC samples, the *p*-value cutoff was selected as 0.05.

The human protein atlas (HPA)

The HPA (<https://www.proteinatlas.org/>) online database [31] was used in the present study to find the subcellular localization of proteins encoded by the hub genes in KIRC cells. This database in-house more than ten million high-

resolution images of the stained tissues with immunohistochemical (IHC) staining. Moreover, this database has also helped to perform hub genes expression and survival analysis at protein level. The *p*-value cutoff was selected as 0.05.

OncoDB

OncoDB [28] is used to visualize relationships among patient clinical information and promoter methylation levels across TCGA datasets. In our study, OncoDB employed to check the DNA promoter methylation level of identified hub genes in KIRC patients. The *p*-value cutoff was selected as 0.05.

cBioPortal

Multidimensional cancer genomic analysis on TCGA cancer datasets is carried out using the cBioPortal, an online open-access platform [32]. This database can query the gene(s) of interest and explore relevant changes across more than 5,000 cancer samples in 20 cancer studies. In this study, a TCGA KIRC dataset, namely, "TCGA PanCancer Atlas (512 cases)", was used for analyzing genetic mutations, mutational hotspots, co-expressed genes, and the effect of mutations on the survival of KIRC patients with default setting.

Functional enrichment analysis

Using the GSEA program, the functional enrichment including GO and KEGG analysis of the hub genes was carried out in this study. Based on the biological phenomena of the examined protein or gene list, this tool identified KEGG and GO terms [33]. The *p*-value cutoff was selected as 0.05.

TIMER database

The web-based TIMER database is utilized to assess the tumor infiltration of immune cells [34]. A variety of algorithms are used in this database to estimate the abundance of immune cells across different cancers. In this research, levels of immune cell infiltration in KIRC were plotted against hub gene expression. The *p*-value cutoff was selected as 0.05.

CancerSEA analysis

CancerSEA was created to decode Pearson correlations between 14 different single-cell

functional states and relevant gene(s) in human malignancies [35]. This database contains gene sequencing profiles of 4043 tumor cells. In this study, we used CancerSEA to investigate the relationships between hub genes and the aforementioned KIRC functional states. The *p*-value cutoff was selected as 0.05.

miRNA network of the hub genes'

The ENCORI database is utilized for exploring miRNA-ncRNA and mRNA-miRNA interactions from CLIP-seq and degradome-seq interaction data [36]. In this investigation, the ENCORI database was used to create the miRNA network of the identified hub genes.

Hub genes' drug prediction analysis

We performed the DrugBank research to find the drugs related to the hub genes because we believe that the identified hub genes can be interesting therapeutic targets. This database offers information on drugs that target hub genes from numerous trustworthy sources [37].

GSCALite is a web-based tool for performing gene set cancer analysis [38]. In this study, we used GSCALite to examine the hub genes' drug sensitivity. This analysis may help us choose better drugs to target the hub genes.

In vitro validation of the hub gene expression and methylation status

Cell culture, RNA, and DNA extraction: Human RCC cell lines (786-O and A-498), and normal renal tubular epithelial cell line (HK-2), provided by the ATCC (American Type Culture Collection) were cultured in DMEM (HyClone), supplemented with 10% fetal bovine serum (FBS; TBD), 1% glutamine, and 1% penicillin-streptomycin in 5% CO₂ at 37°C. RNA extraction from all the cells lines was carried out using TRIzol® reagent method [39], while DNA extraction was done following organic method [40].

RT-qPCR validation analysis: The specific protocols are as follows: First, the PrimeScript™ RT reagent kit (Takara, Japan) was used for reverse transcription of the extracted RNA from HK-2, 786-O, and A-498 cell lines into complementary DNA. Then, the RT-qPCR was carried out on an ABI ViiA 7 Real Time PCR System (Thermo

Fisher, USA) with a SuperReal SYBR Green Premix Plus (Tiangen Biotech, China) as a fluorescent dye. GAPDH was chosen as the internal reference in the present study. All the experiments were in triplicate independently. All the primers of each hub gene are shown as following. The 2-ΔΔCt method was employed to evaluate the relative expression of each hub gene [41].

GAPDHF 5'-ACCCACTCCTCCACCTTTGAC-3, GAPDHR 5'-CTGTTGCTGTAGCCAAATTCG-3 [42]. VEGAF 5'-GGGTGGGCTAGTTAGTGCT, VEGFAR 5'-CCTGTGCTAGGGGATGGAAAT-3' [43]. ALBF 5'-TGAAACATACGTTCCCAAAGAGTTT-3', ALBR 5'-CTCTCCTTCTCAGAAAGTGTGCAT-3' [44]. ENOF 5'-GGCCCTGAGGGCCTCCAAAATCGTAAAAATCATCGG-3', ENOR 5'-GGTCAAAGACAGCTGCATCA-3' [45]. CAV1F 5'-CAGCATGTCTGGGGGCAAT-3', CAV1R 5'-TCAGCTCGTCTGCCATGGCC-3' [46].

Targeted bisulfite-seq analysis: DNA samples were sent to Beijing Genomics Institute (BGI) company for RNA-seq bisulfite-seq analysis. Following targeted bisulfite-seq analysis, methylation values were normalized as beta values. The obtained beta values against hub genes in RCC and normal control cell line were compared to identify differences in the methylation levels.

Statistics analysis

DEGs identified and measurement of methylation and expression levels differences among hub genes across RCC and control cell lines were using a t-test [47]. While for GO and KEGG enrichment analysis, we used Fisher's Exact test for computing statistical difference [48]. Correlational analyses were carried out using Pearson method. For comparisons, a student t-test was adopted in the current study. All the analyses were carried out in R version 3.6.3 software.

Results

Screening of DEGs

Following the standard cutoff criterion (mentioned in the method section), DEGs between KIRC (n = 20) and control samples (n = 20) included in the GSE6344 dataset were found with the use of the "limma" package (**Figure**

KIRC biomarkers

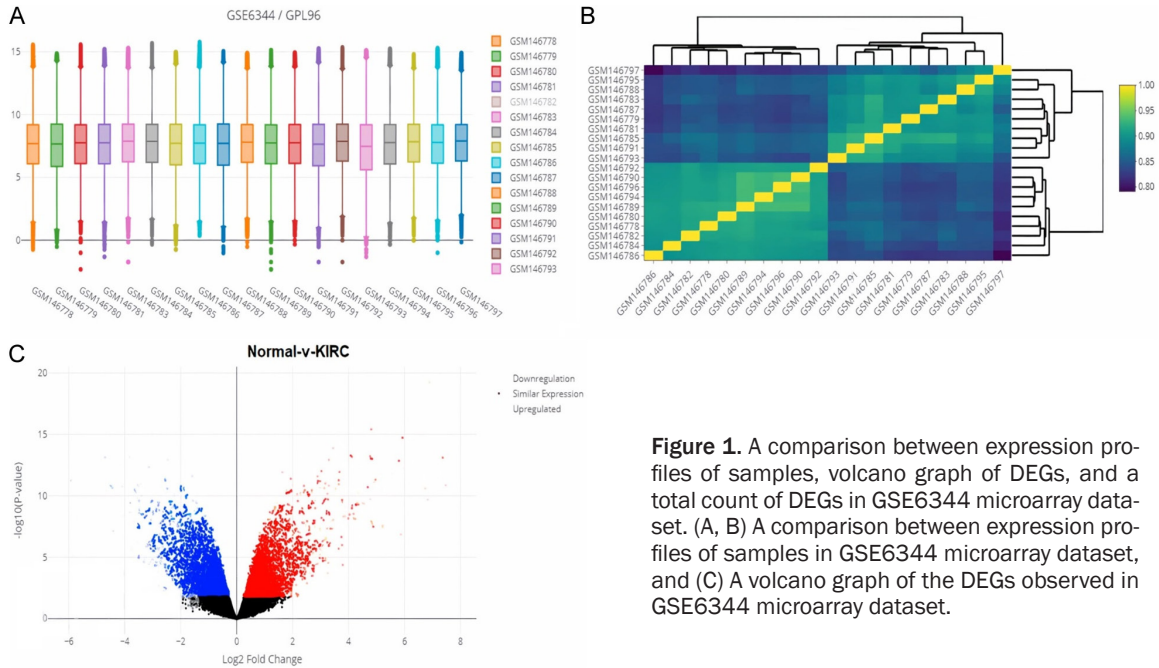


Figure 1. A comparison between expression profiles of samples, volcano graph of DEGs, and a total count of DEGs in GSE6344 microarray dataset. (A, B) A comparison between expression profiles of samples in GSE6344 microarray dataset, and (C) A volcano graph of the DEGs observed in GSE6344 microarray dataset.

1A, 1B). After the identification process was complete, a total of 7299 DEGs were found (**Figure 1C**). The top 250 DEGs in terms of p value were then selected from these 7299 DEGs for further analysis in the current study.

PPI network construction, module identification, and hub genes exploration

After determining a minimum needed interaction score of >0.4 as a threshold, the 250 DEGs were subjected to STRING analysis for PPI construction (**Figure 2A**). There were 763 edges and 250 nodes in the constructed PPI network (**Figure 2A**). Then, within the generated PPI, we determined the most important module in order to screen the top genes linked to KIRC development. As shown in **Figure 2B, 2C**, the identified module was the most significant module in terms of total gene count ($n = 17$). Therefore, we further process this module for hub genes exploration. In order to do this, we integrated the MNC, DMNC, MCC, and Degree of the Cytohubba scoring algorithms [25]. The top four shared DEGs by these 4 algorithms were regarded as hub genes. In total, 4 genes, out of which 3 significantly up-regulated genes, including VEGFA (vascular endothelial growth factor), ALB (Albumin), ENO2 (enolase 2), and one significantly down-regulated gene, CAV1 (Caveolin 1) were regarded as the hub genes (**Figure 2D**).

Hub genes expression profiling at mRNA and protein level in UALCAN

Since four genes (VEGFA, ALB, ENO2, and CAV1) were regarded as hub genes, we then performed the expression analysis of these genes at mRNA and protein level across KIRC samples and normal controls using the UALCAN database. Results highlighted that VEGFA, ENO2, and CAV1 hub genes' expression was up-regulated while the expression ALB hub gene was down-regulated in KIRC samples relative to controls at both mRNA and protein level (**Figure 3A-C**). These results further highlighted that VEGFA, ENO2, and CAV1 expression was also notably higher, while ALB expression was notably lower among KIRC patients of different clinical variables (cancer stage, race, gender, and age group) relative to control samples (**Supplementary Figure 1**). These expression analyses results from the UALCAN database are in line with the expression results of the analyzed dataset (GSE6344).

Verification of the hub genes expression and survival analysis via GEPIA, OncoDB, DriverDBv3, and GENT2 databases

Using the GEPIA, OncoDB, DriverDBv3, and GENT2 databases, we also carried out the expression validation analysis of the hub genes in TCGA datasets and cell lines. As shown in

KIRC biomarkers

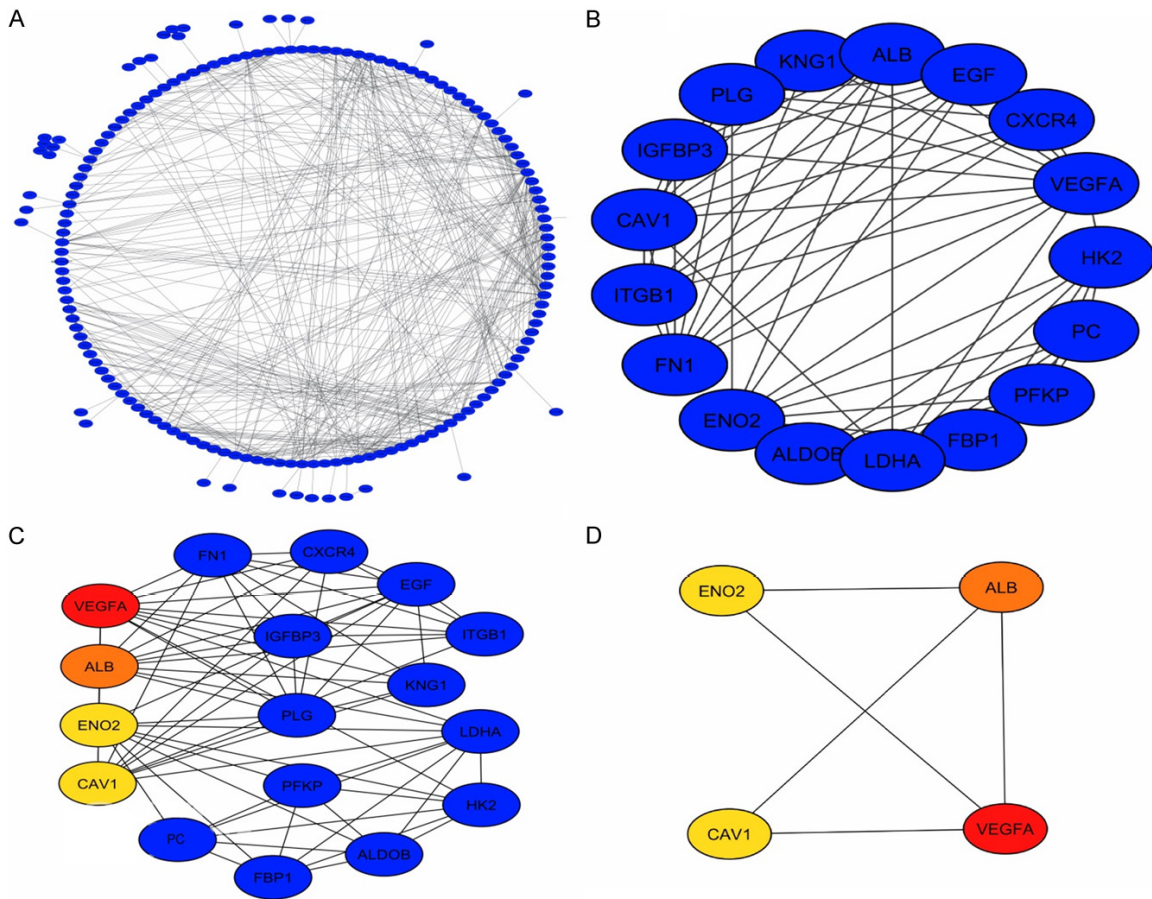


Figure 2. A PPI network of the top 250 DEGs, a significant module in the constructed PPI network, and a PPI network of the identified hub genes in GSE6344 microarray dataset. (A) A PPI network of the top 250 DEGs in GSE6344 microarray dataset, (B, C) A PPI network of the most significant module, and (D) A PPI network of identified four hub genes.

Supplementary Figure 2A-C, the mRNA expression of VEGFA, ENO2, and CAV1 was significantly higher, while the mRNA expression of ALB was lower in KIRC samples relative to normal individuals. Moreover, mRNA expressions of the VEGFA, ENO2, and CAV1 genes were also found to be significantly up-regulated in KIRC cell lines as compared to normal individual cell line via the GENT2 database (Supplementary Figure 2D). This situation makes it clear that in KIRC patients and cell lines, the hub genes VEGFA, ENO2, and CAV1 are considerably over-expressed while ALB is markedly under expressed. Next, we explored the prognostic values of the hub genes (VEGFA, ALB, ENO2, and CAV1) in KIRC patients using via the survival analysis module of the GEPIA database.

Results of the analysis highlighted that the higher expression of VEGFA, ENO2, and CAV1

and the lower expression of ALB were linked with the worst OS of the KIRC patients (Supplementary Figure 2E). Therefore, it is speculated that hub genes may be used as an accurate prognostic model to predict the survival rate of KIRC patients.

Subcellular localization, protein expression validation, and survival analysis of the VEGFA, ALB, ENO2, and CAV1

Through the HPA database, the subcellular location of VEGFA, ALB, ENO2, and CAV1 in KIRC cells was noted. For VEGFA, this protein was mainly enriched in vesicles (Figure 4A), the ALB localization was found Golgi apparatus and endoplasmic reticulum (Figure 4A), ENO2 localization was enriched in the plasma membrane and cytosol (Figure 4A), and CAV1 localization was seen in the Golgi apparatus (Figure 4A). An

KIRC biomarkers

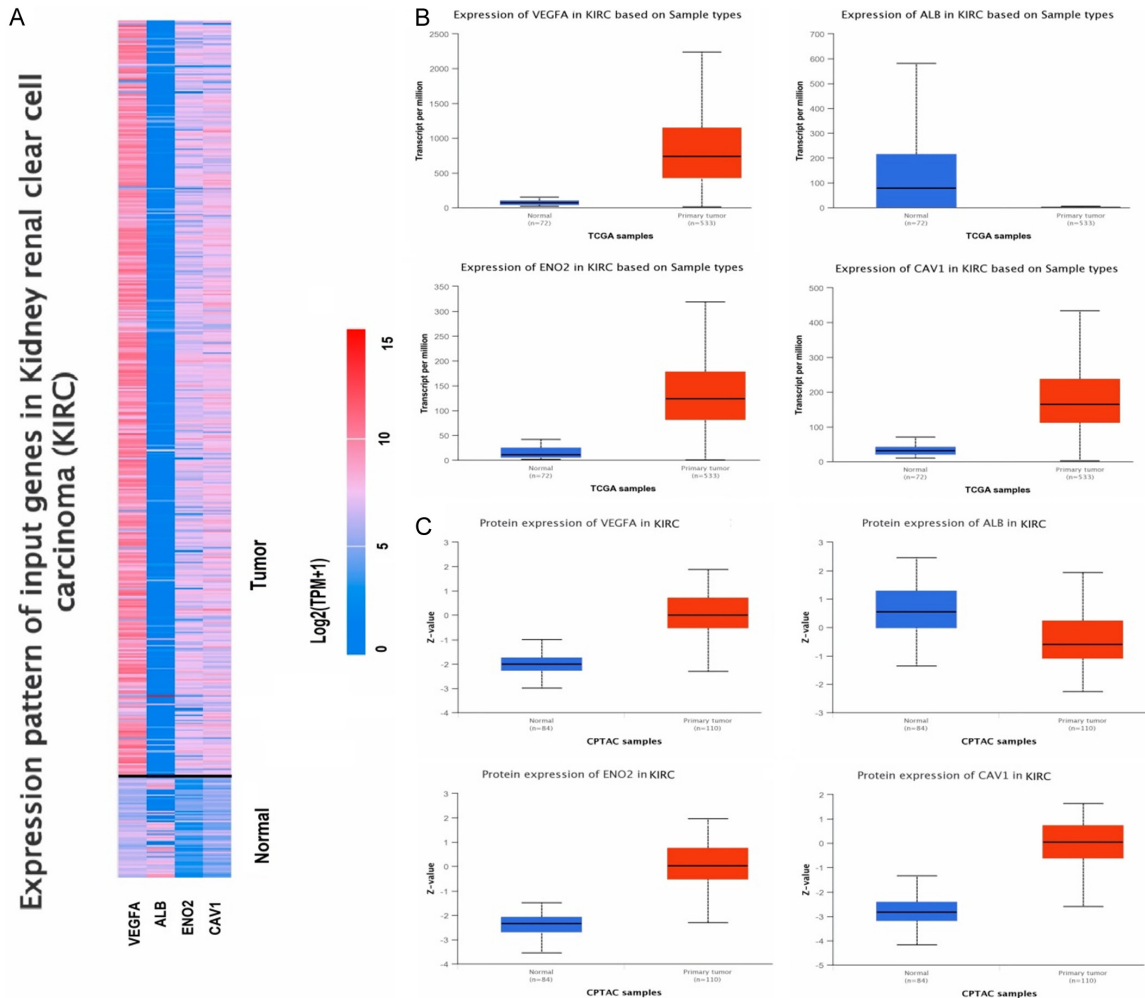


Figure 3. mRNA and protein expression profiling of VEGFA, ALB, ENO2, and CAV1 via UALCAN. (A) A heatmap of VEGFA, ALB, ENO2, and CAV1 hub genes in KIRC sample group and normal control group, (B) Box plot presentation of VEGFA, ALB, ENO2, and CAV1 hub genes mRNA expression in KIRC sample group and normal control group, and (C) Box plot presentation of VEGFA, ALB, ENO2, and CAV1 hub genes protein expression in KIRC sample group and normal control group.

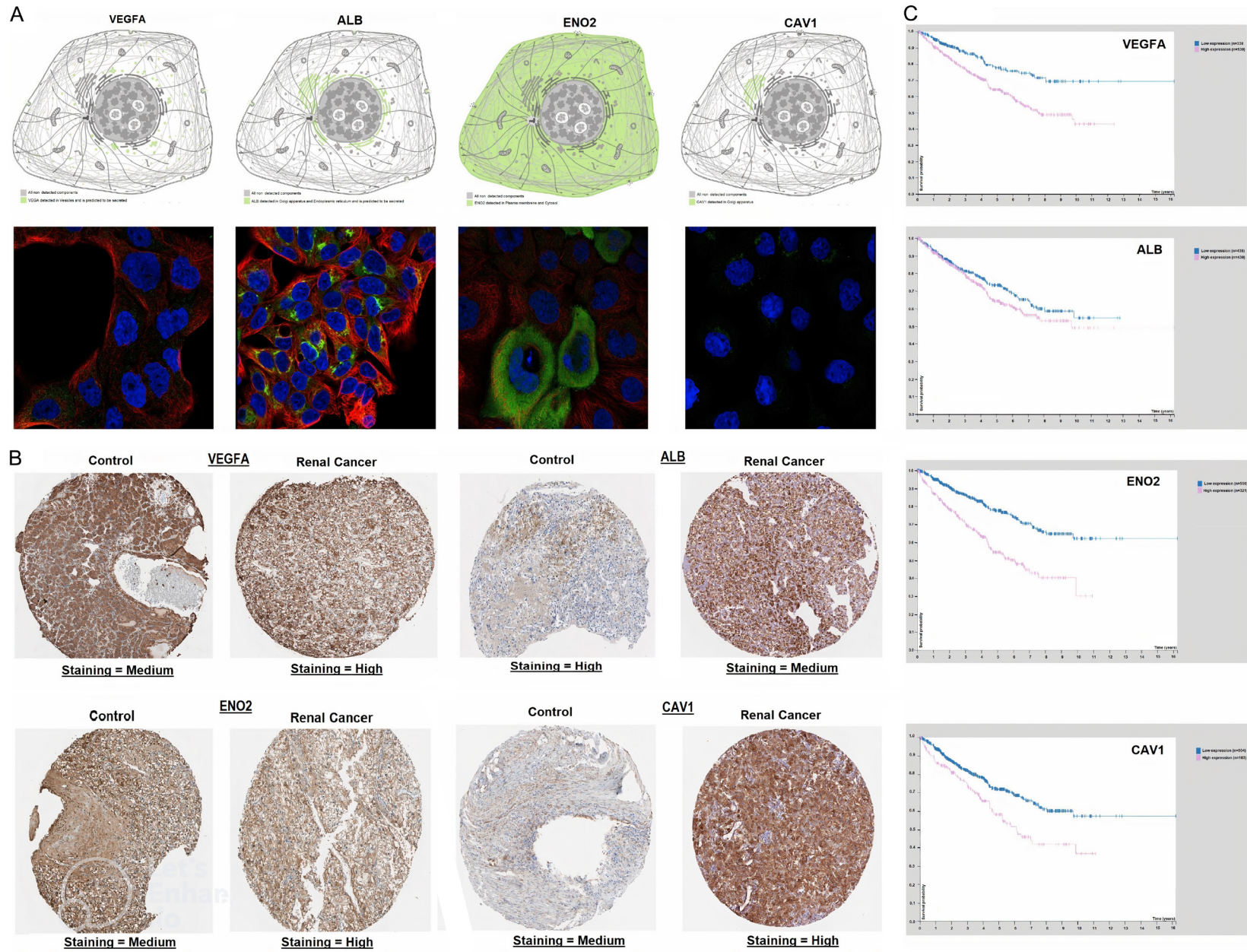
immunohistochemistry (IHC)-based protein expression of the VEGFA, ALB, ENO2, and the CAV1 was analyzed in KIRC samples relative to controls via HPA. As a result, it was noted that the expression of VEGFA, ENO2, and CAV1 was higher (staining = high) in KIRC samples (**Figure 4B**) relative to control samples (staining = medium) (**Figure 4B**), while the expression of ALB was lower (staining = medium) in KIRC samples relative to control (staining = high) (**Figure 4B**). In addition, HPA also helped to analyze the survival outcomes of the hub gene expression at the protein level in KIRC via survival analysis. Results of the survival analysis verified that higher protein expressions of VEGFA, ENO2, and CAV1 are associated with

the poor OS of the KIRC patients. However, ALB survival outcome at protein level were not in line with survival outcome from the GEPIA (**Figure 4C**). The different survival outcomes of ALB in the HPA database may be due to the small sample size of the KIRC datasets as compared to the GEPIA database. Therefore, further studies based on the large KIRC sample size are needed to conduct to verify the survival-related outcomes of the ALB.

Promoter methylation level and expression of VEGFA, ALB, ENO2, and CAV1

We figure out the influence of promoter methylation in the dysregulation of VEGFA, ALB, ENO2,

KIRC biomarkers



KIRC biomarkers

Figure 4. Subcellular localization, protein expression, and survival outcomes' validation of VEGFA, ALB, ENO2, and CAV1 via HPA database. (A) Subcellular localization prediction of VEGFA, ALB, ENO2, and CAV1, (B) Protein expression validation of VEGFA, ALB, ENO2, and CAV1, and (C) Survival outcomes validation of VEGFA, ALB, ENO2, and CAV1.

and CAV1 hub genes' expression in KIRC. Using OncoDB, we explored if the VEGFA, ALB, ENO2, and CAV1 expressions at the mRNA level were regulated by the promoter methylation in KIRC or not. Interestingly, owing to the promoter methylation level, we found a significant hypermethylation of these hub genes' promoters in KIRC specimens compared to controls ([Supplementary Figure 3](#)). Therefore, it is concluded that out of 4 analyzed hub genes, the lower expression of ALB was related to the promoter methylation level, while the higher expression of VEGFA, ALB, and ENO was not associated with promoter methylation levels.

Genetic mutations, mutational hotspots, co-expressed genes, and the effect of mutations on the survival and mRNA expression levels of the hub genes

Genetic mutations, mutational hotspots identification, co-expressed genes, and the effect of mutations on the survival and mRNA expression of VEGFA, ALB, ENO2, and CAV1 hub genes were explored in KIRC patients using cBioPortal database. ALB gene was the most genetically altered gene and was altered in 1.1% samples of 512 analyzed total samples ([Supplementary Figure 4A](#)). The alteration rates of VEGFA, CAV1, and ENO2 were 0.6%, 0.6%, and 0%, respectively, in the analyzed KIRC samples and the deep deletion accounted for most of the changes in VEGFA and CAV1 genes while missense mutations accounted for most of the changes in ALB gene ([Supplementary Figure 4A](#)). Concerning mutational hotspots in proteins encoded by the ALB gene, most of mutation was found to hit the functionally important domains (Serum albumin) of the ALB protein ([Supplementary Figure 4A](#)), out of which A241G was the frequently observed mutation in KIRC. Using the "Survival analysis" feature of the cBioPortal database, we drew the OS and DFS curves of the hub genes between the two sample groups i.e., one group is consisting of those KIRC samples which were genetically altered with hub genes alterations and the second group of those samples which did not have alterations in those hub genes ([Supplementary Figure 4B](#)). Results of the survival analysis

revealed that the genetically altered group of KIRC samples had the worst OS and DFS survival rates relative to the unaltered group of KIRC patients ([Supplementary Figure 4B](#)). Moreover, by performing co-expressed gene analysis, we calculated correlation coefficients and identified that along with VEGFA, ZNF160 was a significant co-expressed gene in KIRC samples ([Supplementary Figure 4C](#)), while APOA2, EFNA3, and CAV2 were the highly co-expressed genes in KIRC samples with ALB, ENO2, and CAV1, respectively ([Supplementary Figure 4C](#)).

Functional enrichment analysis

GO and KEGG enrichment analyses of hub genes (VEGFA, ALB, ENO2, and CAV1) were done with the help of DAVID tool. Cellular components (CC), biological process (BP), and molecular functions (MF) are 3 major functions of the GO enrichment analysis. In this study, Phosphopyruvate hydratase complex, spherical high-density lipoprotein particle, chylomicron, dystrophin-associated glycoprotein complex, and glycoprotein complex, etc., were the major CC of the hub genes ([Supplementary Figure 5A](#)). Vascular endothelial growth factor receptor, 1 binding, high-density lipoprotein particle receptor binding, phosphopyruvate hydratase activity, potassium channel inhibitor activity, etc., BP were mainly associated with hub genes ([Supplementary Figure 5B](#)), while caveola assembly, Neg. reg. of nitric-oxide synthase activity, Reg of cardiac muscle cell action potential involved in reg. of contraction etc., were the primary MFs of the hub genes ([Supplementary Figure 5C](#)). Moreover, KEGG pathways for the identified hub genes are highlighted in [Supplementary Figure 5D](#), and bacterial invasion of epithelial cells, bladder cancer, fluid shear stress and atherosclerosis, HIF-1 signaling pathways were found to be involved in the pathogenesis of KIRC.

Single-cell functional analysis

Hub genes' further involvement in KIRC at single cell level was explored via CancerSEA database. All hub genes including VEGFA, ALB, ENO2, and CAV1 were revealed to be linked (positively or negatively) with fourteen different

KIRC biomarkers

Table 1. DrugBank-based hub genes-associated drugs

Sr. No	Hub gene	Drug name	Effect	Reference	Group
1	VEGFA	Acetaminophen	Decrease expression of VEGFA mRNA	A20420	Approved
		Acetylcysteine		A20451	
		Alvocidib		A20631	
		Cyclosporine		A20661	
		Estradiol		A21103	
2	ALB	Acetaminophen	Increase expression of ALB mRNA	A20426	Approved
		Amiodarone		A20643	
		Cyclosporine		A20661	
		Diclofenac		A22275	
3	ENO2	Estradiol	Decrease expression of ENO2 mRNA	A21098	Approved
		Genistein		A21119	
		Cyclosporine		A20661	
4	CAV1	Cyclosporine	Decrease expression of CAV1 mRNA	A20661	Approved
		Estradiol		A21424	

states at the single cell level in kidney cancer (Supplementary Figure 6A). However, real hub gene expression was notably positively correlated with stemness and angiogenesis (Supplementary Figure 6B).

Immune cells analysis of the hub genes

Next, we further evaluated relationships among different immune cell infiltration (CD8+ T, CD4+ T, and Macrophages) and hub genes (VEGFA, ALB, ENO2, and CAV1) expression via the "TIMER" tool. The VEGFA, ALB, and CAV1 expression was found positively correlated ($P < 0.05$) with the infiltration of CD8+ T, CD4+ T, and Macrophages cells, while ENO2 was explored having a negative correlation ($P < 0.05$) with the immune infiltration of CD8+ T, CD4+ T and Macrophages cells (Supplementary Figure 7).

lncRNA-miRNA-mRNA interaction network

Via ENCORI and Cytoscape, we constructed the lncRNA-miRNA-mRNA co-regulatory networks of VEGFA, ALB, ENO2, and CAV1. In the constructed networks, the total count of lncRNAs, miRNAs, and mRNAs were 31, 252, and 4, respectively (Supplementary Figure 8). Based on the constructed networks, we have identified one miRNA (hsa-mir-107), that targets all hub genes simultaneously. Therefore, we speculate that the identified lncRNAs, hsa-mir-107, and hub genes (VEGFA, ALB, ENO2, and CAV1) (Supplementary Figure 8) as an axis, might also be the potential inducers of the KIRC.

Drug prediction analysis of hub genes

For patients suffering from KIRC, medical treatment is the first option for treatment. Therefore, a selection of appropriate candidate drugs is required. In the current study, via DrugBank database, we explored some potential drugs, that can reverse the gene expression of identified hub genes for the treatment of KIRC. As well, we also analyzed the drug sensitivity of various available drugs against the expression of VEGFA, ALB, ENO2, and CAV1. As a result, it was noted that Estradiol and Cyclosporine drugs along with many other drugs are the negative expression regulators of VEGFA, ENO2, and CAV1, while positive expression regulators of ALB mRNA expression (Table 1).

Experimental in vitro validation of the hub gene methylation status

In the current study, by performing targeted bisulfite-seq analyses of 3 RCC cell lines, including 786-O and A-498, and the normal renal tubular epithelial cell line HK-2, methylation levels of the hub gene were validated. In this analysis, the methylation level was validated using beta values. As shown in Figure 5A, it was noticed that the beta values of the hub genes were lower in normal (HK-2) cell line while higher in the RCC cell line (786-O and A-498) (Figure 5A).

RT-qPCR validation analysis of VEGFA, ALB, ENO2, and CAV1

To confirm our bioinformatics analysis, we conducted an RT-qPCR experiment to measure the

KIRC biomarkers

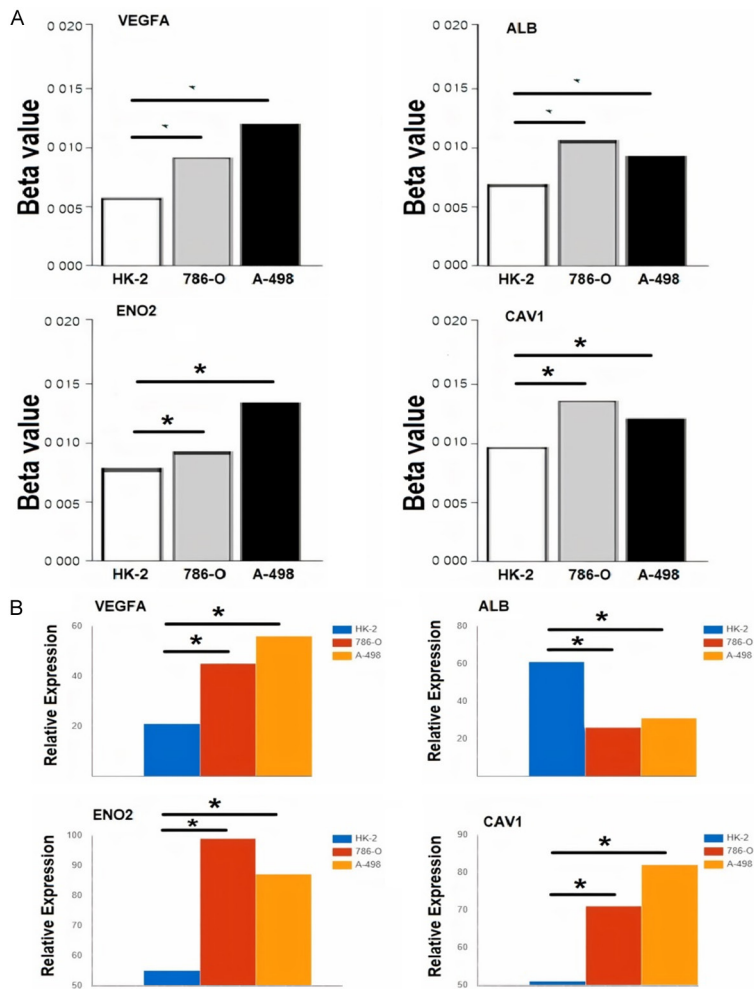


Figure 5. Validating hub gene methylation and expression status using HK-2, 786-O, and A-498 cell lines via targeted bisulfite-seq and RT-qPCR analyses. (A) Beta values based methylation plots of the hub genes, and (B) Relative expression based plots of the hub genes. * $P < 0.05$.

mRNA expression levels the hub genes (VEGFA, ALB, ENO2, and CAV1) in RCC cell lines (786-O and A-498) compared to a normal control cell line (HK-2). Our results, depicted in **Figure 5B**, showed significant differences in the expression levels of all four hub genes between the RCC cell lines and HK-2 control cell line. Notably, VEGFA, ENO2, and CAV1 were up-regulated, while ALB was down-regulated in the RCC cell lines compared to HK-2 (**Figure 5B**), which is consistent with our prediction based on GEO and TCGA datasets analysis.

Discussion

KIRC is one of the most fatal urological malignancies, and its prevalence around the world has been on the rise over the past decades [49]. Due to the heterogeneous nature of the

KIRC, the mechanisms governing its development, progression, and metastasis are very complex and poorly understood [50]. Therefore, revealing key genes associated with the pathogenesis, prognosis, and metastasis of KIRC is very important. In the present study, we analyzed the GSE-6344 [18] microarray dataset from the GEO database to unveil DEGs among the KIRC patients group and normal individuals group, in order to identify hub genes as reliable novel biomarkers in KIRC patients. In addition to this, a few important parameters (promoter methylation level, genetic alterations, and sub-cellular localization, etc.) associated with the hub genes were also analyzed in the present study. Moreover, we also identified different chemotherapeutic drugs that could alter the expression of hub genes to treat KIRC, aiming to open new avenues for the development of novel treatment strategies for KIRC in the future.

After the identification process, a total of 7299 DEGs were found between the KIRC and normal groups. The top 250 DEGs in terms of p -value were then selected from these 7299 DEGs for further analysis in the current study. After constructing the PPI, and module analysis of the identified top 250 DEGs, the identified hub genes VEGFA, ENO2, and CAV1 were significantly up-regulated, while ALB was significantly down-regulated in KIRC samples relative to normal tissues. Moreover, we also utilized different TCGA expression-based databases and HPA to further validate the results of GEO expression analysis. Similar to GEO expression analysis results, the findings of additional databases further confirmed the significant up-regulation of VEGFA, ENO2, and CAV1 and the down-regulation of ALB among the KIRC samples group and the normal samples group.

The VEGFA gene encodes for angiogenic factors, which can affect the microenvironment inside endothelial cells for initiating the angiogenesis process [51]. Across various tumors, the higher expression of VEGFA was not only found to initiate tumor development, progression, and metastasis but also causing the stimulation of hemopoietic and endothelial cells [52-54]. A previous study reported that hypoxia is the stimulator of VEGFA higher expression across cancerous cells [55]. *Wong et al.* revealed that in glioblastoma (GBM) cells, the higher expression of VEGFA was associated with the enrichment of blood vessels [56]. *Gong et al.* highlighted that VEGFA overexpression is also associated with the expression regulation of matrix metalloproteinase 2 (MMP2), which is a major factor in cancer invasiveness [57]. This study also suggested that MMP2 down-regulation with appropriate chemotherapeutic drugs could be helpful in the inhibition of the angiogenesis process across cancer cells [57].

In routine clinical practice, the ALB detection index is the liver function test and is associated with the nutritional status of the patient [58], especially that of cancer patients [59]. Previous studies reported the involvement of ALB in a variety of cancer initiation mechanisms and treatment. For example, the concentration of ALB in serum is useful to reflect the status of chronic inflammation. Recent studies reported that ALB synthesis is significantly lower during cancer-associated systemic inflammation caused by different cytokines and growth factors [60, 61]. Furthermore, lower ALB expression was also found to be involved in antioxidant and anticancer effects [61, 62].

ENO2 is mainly expressed in different kind of cells, including nerve cells, red blood cells, breast tissue cells, prostate cells, platelets, and uterus cells [63, 64]. ENO2 has been reported to be overexpressed in gastric, prostate, and different other types of human cancers [65, 66]. According to a study conducted by *Yan et al.*, ENO2 expression was notably higher in hypoxic and glioma cells [66]. This research further proposed that the silencing of ENO2 expression with appropriate drugs can inhibit cell growth in the gliomas. Moreover, currently published studies are mainly focused on the biomarker potential of ENO2 expression

in cancer patients [63]. In this regard, it was observed that higher ENO2 expression may be a useful diagnostic and prognostic biomarker as well as a reliable therapeutic target for treating cancer patients. *Liu et al.* reported that, by enhancing the Akt activity, the ENO2 overexpression is associated with the initiation of cell proliferation, and glucocorticoid tolerance among acute lymphocytic leukemia (ALL) patients [67].

Depending on the cancer stage, CAV1 plays a dual role, i.e., a tumor suppressor and a metastasis initiator role in cancer cells [68]. In addition to this, CAV1 overexpression was found to promote the migration of cancer-derived cells by unknown mechanisms [69]. As well, the higher expression of CAV1 favors cancer development, progression, invasion, and metastasis [70, 71]. Contrary to this, CAV1 down-regulation was also found to be associated with the development of different cancers, such as lung cancer [72], colon cancer [73], and ovarian cancer [74]. In a nutshell, these findings showed that CAV1 displays tumor suppressor as well as oncogenic properties in a variety of cancer models.

More importantly, the identified hub genes were also found to be significant for predicting the OS of KIRC patients. The higher expression of VEGFA, ENO2, and CAV1 while lower expression of ALB was linked with the worst OS of KIRC patients. Therefore, these hub genes can be used as an accurate prognostic model to predict the OS of KIRC patients. The protein expression (immunohistochemical staining) results via the HPA database further showed that hub gene proteins' expression was consistent (high) with their mRNA expression level. This validation of mRNA and protein expression at both levels further enhanced the accuracy of the identified hub genes as molecular biomarkers. To our knowledge, no studies have reported the role of these four hub genes in the initiation and progression of KIRC. In terms of the mutational and methylation statuses of the VEGFA, ALB, ENO2, and CAV1 genes, it was discovered that these genes are not prone to genetic mutations in KIRC, while the lower expression of ALB was connected to the promoter methylation of this gene. However, the increased levels of VEGFA, ALB, and ENO2 expression in KIRC were not associated with promoter methylation.

To further enhance the understanding of these hub genes' pathogenic role in the development of KIRC, we next revealed that VEGFA, ALB, ENO2, and CAV1 hub genes were involved in a variety of GO terms and participate in various cancer-associated signaling pathways, such as bacterial invasion of epithelial cells, bladder cancer, fluid shear stress, and atherosclerosis, as well as HIF-1 signaling pathways in KIRC patients. The oncogenic roles of these pathways have earlier been well-acknowledged in cancer development [75, 76]. We further noticed that VEGFA, ALB, ENO2, and CAV1 hub genes' expression was regulated simultaneously by hsa-mir-107 miRNA in KIRC patients, and the expressions of these genes was significantly related to the immune cell infiltration of CD8+ T, CD4+ T, and macrophages. Previously, the dysregulation of miR-107 in multiple human cancers has been reported in published studies, for example in breast cancer, bladder cancer, glioblastoma, and esophageal cancer [77-80]. However, any tumor suppressor or tumor-causing role of miR-107 in KIRC is not reported anywhere. Therefore, to the best of our knowledge, this study is the first to report the probable cancer-driving role of the hsa-mir-107 miRNA with respect to VEGFA, ALB, ENO2, and CAV1 hub genes in KIRC.

One of the primary factors that significantly contributes to the importance of this study is the rigorous validation process we employed. We went beyond relying solely on GSE6344 outcomes by validating the expression of hub genes using multiple datasets from The Cancer Genome Atlas (TCGA) and renal cell carcinoma (RCC) cell lines. This comprehensive validation enhances the reliability and robustness of our findings. As a result, the hub genes identified in our study can be considered more reliable compared to similar works. The validation across diverse datasets and cell lines strengthens the confidence in the identified hub genes. However, there were still some limitations: First, besides RNA-seq analysis, more validation analysis, such as real-time quantitative (RT-qPCR) and target-based bisulfite sequencing should be performed using clinical samples from the KIRC patients. Secondly, due to in silico prediction, we are unable to explain that exactly how VEGFA, ALB, ENO2, and CAV1 hub gene-miRNAs networks and therapeutic drugs play a role in the diagnosis and treatment of

KIRC. Thirdly, a detailed conclusive study containing the underlying mechanism, and the biological effect should be carried out in the near future.

Conclusion

Through this detailed study, we proposed a model of four novel hub genes related to the occurrence of KIRC. Hub genes in the proposed model may be exploited as reliable potential biomarkers for the diagnosis, prognosis, and treatment of KIRC patients. However, further comprehensive studies should be conducted to explore the vital pathogenic roles of these genes in KIRC.

Disclosure of conflict of interest

None.

Address correspondence to: Jingyu Zhang, Central People's Hospital of Zhanjiang, Zhanjiang, Guangdong, China. E-mail: yfyxxzjy@bjmu.edu.cn

References

- [1] Cairns P. Renal cell carcinoma. *Cancer Biomark* 2010; 9: 461-473.
- [2] Bray F, Ferlay J, Soerjomataram I, Siegel RL, Torre LA and Jemal A. Global cancer statistics 2018: GLOBOCAN estimates of incidence and mortality worldwide for 36 cancers in 185 countries. *CA Cancer J Clin* 2018; 68: 394-424.
- [3] Valle JW, Borbath I, Khan SA, Huguet F, Gruenberger T and Arnold D; ESMO Guidelines Committee. Biliary cancer: ESMO clinical practice guidelines for diagnosis, treatment and follow-up. *Ann Oncol* 2016; 27 Suppl 5: v28-v37.
- [4] Hsieh JJ, Le V, Cao D, Cheng EH and Creighton CJ. Genomic classifications of renal cell carcinoma: a critical step towards the future application of personalized kidney cancer care with pan-omics precision. *J Pathol* 2018; 244: 525-537.
- [5] Weaver C, Bin Satter K, Richardson KP, Tran LKH, Tran PMH and Purohit S. Diagnostic and prognostic biomarkers in renal clear cell carcinoma. *Biomedicines* 2022; 10: 2953.
- [6] Zhang C, Li Y, Qian J, Zhu Z, Huang C, He Z, Zhou L and Gong Y. Identification of a claudin-low subtype in clear cell renal cell carcinoma with implications for the evaluation of clinical outcomes and treatment efficacy. *Front Immunol* 2022; 13: 1020729.

KIRC biomarkers

- [7] Linehan WM. Genetic basis of kidney cancer: role of genomics for the development of disease-based therapeutics. *Genome Res* 2012; 22: 2089-2100.
- [8] Shuch B, Amin A, Armstrong AJ, Eble JN, Ficarra V, Lopez-Beltran A, Martignoni G, Rini BI and Kutikov A. Understanding pathologic variants of renal cell carcinoma: distilling therapeutic opportunities from biologic complexity. *Eur Urol* 2015; 67: 85-97.
- [9] Chowdhury B, Porter EG, Stewart JC, Ferreira CR, Schipma MJ and Dykhuizen EC. PBRM1 regulates the expression of genes involved in metabolism and cell adhesion in renal clear cell carcinoma. *PLoS One* 2016; 11: e0153718.
- [10] Ahmad M, Hameed Y, Khan M, Usman M, Rehman A, Abid U, Asif R, Ahmed H, Hussain MS, Rehman JU, Asif HM, Arshad R, Atif M, Hadi A, Sarfraz U and Khurshid U. Up-regulation of GINS1 highlighted a good diagnostic and prognostic potential of survival in three different subtypes of human cancer. *Braz J Biol* 2021; 84: e250575.
- [11] McGuire BB and Fitzpatrick JM. Biomarkers in renal cell carcinoma. *Curr Opin Urol* 2009; 19: 441-446.
- [12] Demandt JAF, Dubois LJ, van Kuijk K, Zaťovičová M, Jin H, Parkkila S, van der Laan SW, Jelenska L, Mees BME, Reutelingsperger CPM, Cleutjens KBJM, van der Kallen CJH, Schalkwijk CG, van Greevenbroek MMJ, Biessen EAL, Pasterkamp G, Pastoreková S, Stehouwer CDA and Sluimer JC. The hypoxia-sensor carbonic anhydrase IX affects macrophage metabolism, but is not a suitable biomarker for human cardiovascular disease. *Sci Rep* 2021; 11: 425.
- [13] Sial N, Saeed S, Ahmad M, Hameed Y, Rehman A, Abbas M, Asif R, Ahmed H, Hussain MS, Rehman JU, Atif M and Khan MR. Multi-omics analysis identified TMED2 as a shared potential biomarker in six subtypes of human cancer. *Int J Gen Med* 2021; 14: 7025-7042.
- [14] Sun G, Li Y, Peng Y, Lu D, Zhang F, Cui X, Zhang Q and Li Z. Identification of differentially expressed genes and biological characteristics of colorectal cancer by integrated bioinformatics analysis. *J Cell Physiol* 2019; 234: 15215-15224.
- [15] Yan X, Wan H, Hao X, Lan T, Li W, Xu L, Yuan K and Wu H. Importance of gene expression signatures in pancreatic cancer prognosis and the establishment of a prediction model. *Cancer Manag Res* 2019; 11: 273-283.
- [16] Usman M, Hameed Y, Ahmad M, Iqbal MJ, Maryam A, Mazhar A, Naz S, Tanveer R, Saeed H, Bint-E-Fatima, Ashraf A, Hadi A, Hameed Z, Tariq E and Aslam AS. SHMT2 is associated with tumor purity, CD8+ T immune cells infiltration, and a novel therapeutic target in four different human cancers. *Curr Mol Med* 2023; 23: 161-176.
- [17] Usman M, Hameed Y, Ahmad M, Jalil Ur Rehman, Ahmed H, Hussain MS, Asif R, Murtaza MG, Jawad MT and Iqbal MJ. Breast cancer risk and human papillomavirus infection: a Bradford Hill criteria based evaluation. *Infect Disord Drug Targets* 2022; 22: e200122200389.
- [18] Gumz ML, Zou H, Kreinest PA, Childs AC, Belmonte LS, LeGrand SN, Wu KJ, Luxon BA, Sinha M, Parker AS, Sun LZ, Ahlquist DA, Wood CG and Copland JA. Secreted frizzled-related protein 1 loss contributes to tumor phenotype of clear cell renal cell carcinoma. *Clin Cancer Res* 2007; 13: 4740-4749.
- [19] Cheng Y, Sun M, Wang F, Geng X and Wang F. Identification of hub genes related to Alzheimer's disease and major depressive disorder. *Am J Alzheimers Dis Other Demen* 2021; 36: 15333175211046123.
- [20] Ritchie ME, Phipson B, Wu D, Hu Y, Law CW, Shi W and Smyth GK. Limma powers differential expression analyses for RNA-sequencing and microarray studies. *Nucleic Acids Res* 2015; 43: e47.
- [21] von Mering C, Huynen M, Jaeggi D, Schmidt S, Bork P and Snel B. STRING: a database of predicted functional associations between proteins. *Nucleic Acids Res* 2003; 31: 258-261.
- [22] Bandettini WP, Kellman P, Mancini C, Booker OJ, Vasu S, Leung SW, Wilson JR, Shanbhag SM, Chen MY and Arai AE. MultiContrast Delayed Enhancement (MCOE) improves detection of subendocardial myocardial infarction by late gadolinium enhancement cardiovascular magnetic resonance: a clinical validation study. *J Cardiovasc Magn Reson* 2012; 14: 83.
- [23] Demchak B, Hull T, Reich M, Liefeld T, Smoot M, Ideker T and Mesirov JP. Cytoscape: the network visualization tool for GenomeSpace workflows. *F1000Res* 2014; 3: 151.
- [24] Chin CH, Chen SH, Wu HH, Ho CW, Ko MT and Lin CY. CytoHubba: identifying hub objects and sub-networks from complex interactome. *BMC Syst Biol* 2014; 8 Suppl 4: S11.
- [25] Pan X, Chen S, Chen X, Ren Q, Yue L, Niu S, Li Z, Zhu R, Chen X, Jia Z, Zhen R and Ban J. UTP14A, DKC1, DDX10, PinX1, and ESF1 modulate cardiac angiogenesis leading to obesity-induced cardiac injury. *J Diabetes Res* 2022; 2022: 2923291.
- [26] Chandrashekar DS, Bashel B, Balasubramanya SAH, Creighton CJ, Ponce-Rodriguez I, Chakravarthi BVSK and Varambally S. UALCAN: a portal for facilitating tumor subgroup gene expression and survival analyses. *Neoplasia* 2017; 19: 649-658.

KIRC biomarkers

- [27] Tang Z, Li C, Kang B, Gao G, Li C and Zhang Z. GEPIA: a web server for cancer and normal gene expression profiling and interactive analyses. *Nucleic Acids Res* 2017; 45: W98-W102.
- [28] Tang G, Cho M and Wang X. OncoDB: an interactive online database for analysis of gene expression and viral infection in cancer. *Nucleic Acids Res* 2022; 50: D1334-D1339.
- [29] Liu SH, Shen PC, Chen CY, Hsu AN, Cho YC, Lai YL, Chen FH, Li CY, Wang SC, Chen M, Chung IF and Cheng WC. DriverDBv3: a multi-omics database for cancer driver gene research. *Nucleic Acids Res* 2020; 48: D863-D870.
- [30] Park SJ, Yoon BH, Kim SK and Kim SY. GENT2: an updated gene expression database for normal and tumor tissues. *BMC Med Genomics* 2019; 12 Suppl 5: 101.
- [31] Thul PJ and Lindskog C. The human protein atlas: a spatial map of the human proteome. *Protein Sci* 2018; 27: 233-244.
- [32] Gao J, Aksoy BA, Dogrusoz U, Dresdner G, Gross B, Sumer SO, Sun Y, Jacobsen A, Sinha R, Larsson E, Cerami E, Sander C and Schultz N. Integrative analysis of complex cancer genomics and clinical profiles using the cBioPortal. *Sci Signal* 2013; 6: p11.
- [33] Subramanian A, Tamayo P, Mootha VK, Mukherjee S, Ebert BL, Gillette MA, Paulovich A, Pomeroy SL, Golub TR, Lander ES and Mesirov JP. Gene set enrichment analysis: a knowledge-based approach for interpreting genome-wide expression profiles. *Proc Natl Acad Sci U S A* 2005; 102: 15545-15550.
- [34] Li T, Fan J, Wang B, Traugh N, Chen Q, Liu JS, Li B and Liu XS. TIMER: a web server for comprehensive analysis of tumor-infiltrating immune cells. *Cancer Res* 2017; 77: e108-e110.
- [35] Yuan H, Yan M, Zhang G, Liu W, Deng C, Liao G, Xu L, Luo T, Yan H, Long Z, Shi A, Zhao T, Xiao Y and Li X. CancerSEA: a cancer single-cell state atlas. *Nucleic Acids Res* 2019; 47: D900-D908.
- [36] Huang DP, Zeng YH, Yuan WQ, Huang XF, Chen SQ, Wang MY, Qiu YJ and Tong GD. Bioinformatics analyses of potential miRNA-mRNA regulatory axis in HBV-related hepatocellular carcinoma. *Int J Med Sci* 2021; 18: 335-346.
- [37] Freshour SL, Kiwala S, Cotto KC, Coffman AC, McMichael JF, Song JJ, Griffith M, Griffith OL and Wagner AH. Integration of the drug-gene interaction database (DGldb 4.0) with open crowdsource efforts. *Nucleic Acids Res* 2021; 49: D1144-D1151.
- [38] Liu CJ, Hu FF, Xia MX, Han L, Zhang Q and Guo AY. GSCALite: a web server for gene set cancer analysis. *Bioinformatics* 2018; 34: 3771-3772.
- [39] Rio DC, Ares M Jr, Hannon GJ and Nilsen TW. Purification of RNA using TRIzol (TRI reagent). *Cold Spring Harb Protoc* 2010; 2010: pdb.prot5439.
- [40] Ghatak S, Muthukumaran RB and Nachimuthu SK. A simple method of genomic DNA extraction from human samples for PCR-RFLP analysis. *J Biomol Tech* 2013; 24: 224-231.
- [41] Livak KJ and Schmittgen TD. Analysis of relative gene expression data using real-time quantitative PCR and the 2^{-Delta Delta C(T)} method. *Methods* 2001; 25: 402-408.
- [42] Jafri HSMO, Mushtaq S and Baig S. Detection of Kras gene in colorectal cancer patients through liquid biopsy: a cost-effective method. *J Coll Physicians Surg Pak* 2021; 31: 1174-1178.
- [43] Mushimiyimana I, Tomas Bosch V, Niskanen H, Downes NL, Moreau PR, Hartigan K, Ylä-Herttuala S, Laham-Karam N and Kaikkonen MU. Genomic landscapes of noncoding RNAs regulating VEGFA and VEGFC expression in endothelial cells. *Cell Mol Biol* 2021; 41: e0059420.
- [44] Yang Q, Ali HA, Yu S, Zhang L, Li X, Du Z and Zhang G. Evaluation and validation of the suitable control genes for quantitative PCR studies in plasma DNA for non-invasive prenatal diagnosis. *Int J Mol Med* 2014; 34: 1681-1687.
- [45] Usui Y, Hirasawa T, Furusawa C, Shirai T, Yamamoto N, Mori H and Shimizu H. Investigating the effects of perturbations to *pgi* and *eno* gene expression on central carbon metabolism in *Escherichia coli* using (13)C metabolic flux analysis. *Microb Cell Fact* 2012; 11: 87.
- [46] Pietrzak J, Szmajda-Krygier D, Wosiak A, Świechowski R, Michalska K, Mirowski M, Żebrowska-Nawrocka M, Łochowski M and Balcerczak E. Changes in the expression of membrane type-matrix metalloproteinases genes (MMP14, MMP15, MMP16, MMP24) during treatment and their potential impact on the survival of patients with non-small cell lung cancer (NSCLC). *Biomed Pharmacother* 2022; 146: 112559.
- [47] Kim TK. T test as a parametric statistic. *Korean J Anesthesiol* 2015; 68: 540-546.
- [48] Kim HY. Statistical notes for clinical researchers: Chi-squared test and Fisher's exact test. *Restor Dent Endod* 2017; 42: 152-155.
- [49] Hsieh JJ, Purdue MP, Signoretti S, Swanton C, Albiges L, Schmidinger M, Heng DY, Larkin J and Ficarra V. Renal cell carcinoma. *Nat Rev Dis Primers* 2017; 3: 17009.
- [50] Fares J, Fares MY, Khachfe HH, Salhab HA and Fares Y. Molecular principles of metastasis: a hallmark of cancer revisited. *Signal Transduct Target Ther* 2020; 5: 28.
- [51] Bergers G and Benjamin LE. Tumorigenesis and the angiogenic switch. *Nat Rev Cancer* 2003; 3: 401-410.

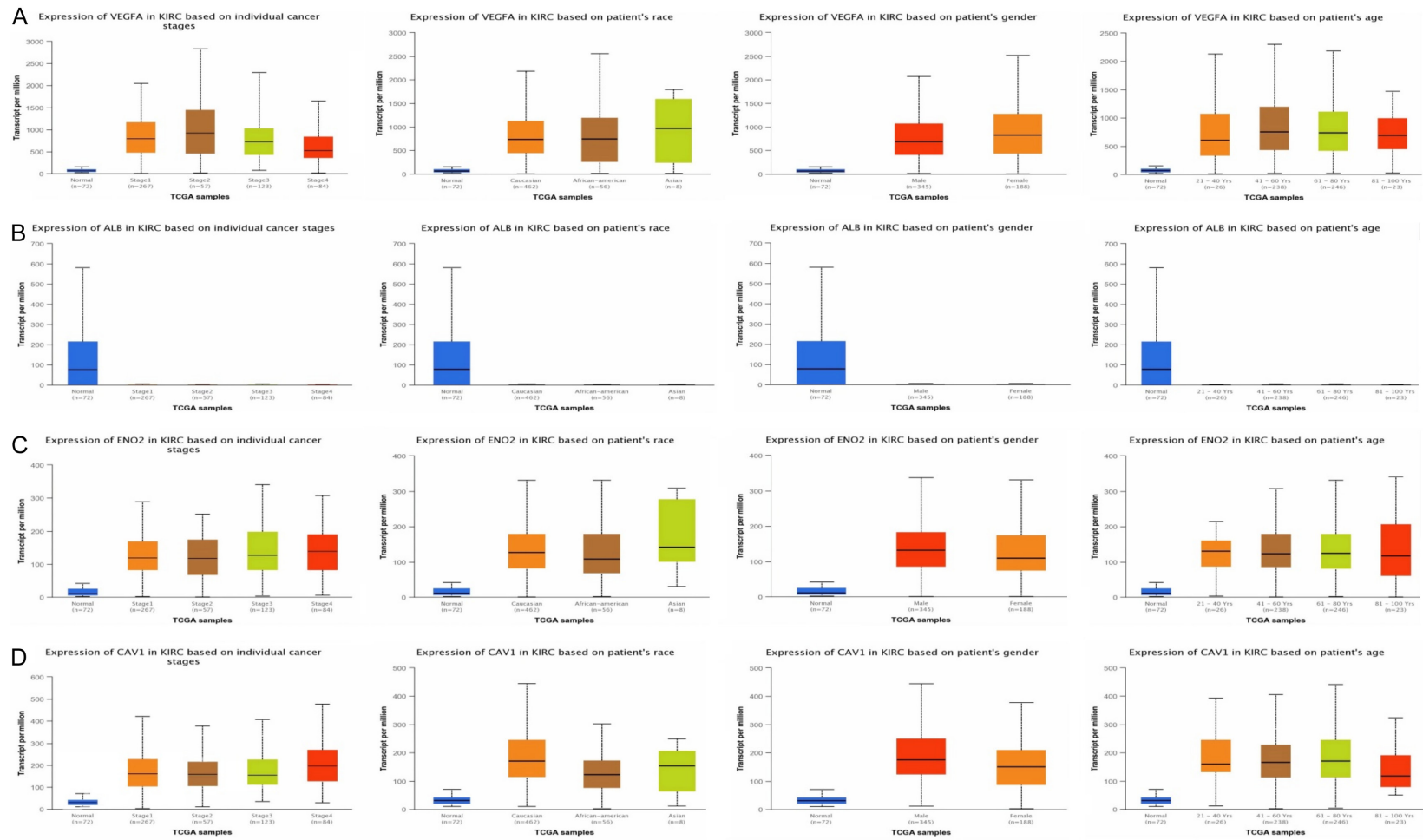
KIRC biomarkers

- [52] Wu Y, Hooper AT, Zhong Z, Witte L, Bohlen P, Raffi S and Hicklin DJ. The vascular endothelial growth factor receptor (VEGFR-1) supports growth and survival of human breast carcinoma. *Int J Cancer* 2006; 119: 1519-1529.
- [53] Kane NM, Xiao Q, Baker AH, Luo Z, Xu Q and Emanuelli C. Pluripotent stem cell differentiation into vascular cells: a novel technology with promises for vascular re(eneration). *Pharmacol Ther* 2011; 129: 29-49.
- [54] Calvo CF, Fontaine RH, Soueid J, Tammela T, Makinen T, Alfaro-Cervello C, Bonnaud F, Miguez A, Benhaim L, Xu Y, Barallobre MJ, Moutkine I, Lyytikka J, Tatlisumak T, Pytowski B, Zalc B, Richardson W, Kessaris N, Garcia-Verdugo JM, Alitalo K, Eichmann A and Thomas JL. Vascular endothelial growth factor receptor 3 directly regulates murine neurogenesis. *Genes Dev* 2011; 25: 831-844.
- [55] Desbaillets I, Diserens AC, Tribolet N, Hamou MF and Van Meir EG. Upregulation of interleukin 8 by oxygen-deprived cells in glioblastoma suggests a role in leukocyte activation, chemotaxis, and angiogenesis. *J Exp Med* 1997; 186: 1201-1212.
- [56] Wong ML, Prawira A, Kaye AH and Hovens CM. Tumour angiogenesis: its mechanism and therapeutic implications in malignant gliomas. *J Clin Neurosci* 2009; 16: 1119-1130.
- [57] Gong J, Zhu S, Zhang Y and Wang J. Interplay of VEGFa and MMP2 regulates invasion of glioblastoma. *Tumour Biol* 2014; 35: 11879-11885.
- [58] Margaron M and Soni N. Serum albumin: touchstone or totem? *Anaesthesia* 1998; 53: 789-803.
- [59] McMillan DC, Watson WS, O’Gorman P, Preston T, Scott HR and McArdle CS. Albumin concentrations are primarily determined by the body cell mass and the systemic inflammatory response in cancer patients with weight loss. *Nutr Cancer* 2001; 39: 210-213.
- [60] Elinav E, Nowarski R, Thaiss CA, Hu B, Jin C and Flavell RA. Inflammation-induced cancer: crosstalk between tumours, immune cells and microorganisms. *Nat Rev Cancer* 2013; 13: 759-771.
- [61] Laursen I, Briand P and Lykkesfeldt AE. Serum albumin as a modulator on growth of the human breast cancer cell line, MCF-7. *Anticancer Res* 1990; 10: 343-351.
- [62] Seaton K. Albumin concentration controls cancer. *J Natl Med Assoc* 2001; 93: 490-3.
- [63] Isgrò MA, Bottoni P and Scatena R. Neuron-specific enolase as a biomarker: biochemical and clinical aspects. *Adv Exp Med Biol* 2015; 867: 125-143.
- [64] Vizin T and Kos J. Gamma-enolase: a well-known tumour marker, with a less-known role in cancer. *Radiol Oncol* 2015; 49: 217-226.
- [65] Park T, Lee YJ, Jeong SH, Choi SK, Jung EJ, Ju YT, Jeong CY, Park M, Hah YS, Yoo J, Ha WS, Hong SC and Ko GH. Overexpression of neuron-specific enolase as a prognostic factor in patients with gastric cancer. *J Gastric Cancer* 2017; 17: 228-236.
- [66] Yan T, Skaftnesmo KO, Leiss L, Sleire L, Wang J, Li X and Enger PØ. Neuronal markers are expressed in human gliomas and NSE knock-down sensitizes glioblastoma cells to radiotherapy and temozolomide. *BMC Cancer* 2011; 11: 524.
- [67] Liu CC, Wang H, Wang WD, Wang L, Liu WJ, Wang JH, Geng QR and Lu Y. ENO2 promotes cell proliferation, glycolysis, and glucocorticoid-resistance in acute lymphoblastic leukemia. *Cell Physiol Biochem* 2018; 46: 1525-1535.
- [68] Nunez-Wehinger S, Ortiz RJ, Diaz N, Diaz J, Lobos-Gonzalez L and Quest AF. Caveolin-1 in cell migration and metastasis. *Curr Mol Med* 2014; 14: 255-274.
- [69] Díaz J, Mendoza P, Ortiz R, Díaz N, Leyton L, Stupack D, Quest AF and Torres VA. Rab5 is required in metastatic cancer cells for Caveolin-1-enhanced Rac1 activation, migration and invasion. *J Cell Sci* 2014; 127: 2401-2406.
- [70] Quest AF, Lobos-Gonzalez L, Nunez S, Sanhueza C, Fernández JG, Aguirre A, Rodríguez D, Leyton L and Torres V. The caveolin-1 connection to cell death and survival. *Curr Mol Med* 2013; 13: 266-281.
- [71] Campos A, Burgos-Ravanel R, González MF, Huilcaman R, Lobos González L and Quest AFG. Cell intrinsic and extrinsic mechanisms of caveolin-1-enhanced metastasis. *Biomolecules* 2019; 9: 314.
- [72] Racine C, Bélanger M, Hirabayashi H, Boucher M, Chakir J and Couet J. Reduction of caveolin 1 gene expression in lung carcinoma cell lines. *Biochem Biophys Res Commun* 1999; 255: 580-586.
- [73] Bender FC, Reymond MA, Bron C and Quest AF. Caveolin-1 levels are down-regulated in human colon tumors, and ectopic expression of caveolin-1 in colon carcinoma cell lines reduces cell tumorigenicity. *Cancer Res* 2000; 60: 5870-5878.
- [74] Wiechen K, Diatchenko L, Agoulnik A, Scharff KM, Schober H, Arlt K, Zhumabayeva B, Siebert PD, Dietel M, Schäfer R and Sers C. Caveolin-1 is down-regulated in human ovarian carcinoma and acts as a candidate tumor suppressor gene. *Am J Pathol* 2001; 159: 1635-1643.

KIRC biomarkers

- [75] Xiong W, Zhong J, Li Y, Li X, Wu L and Zhang L. Identification of pathologic grading-related genes associated with kidney renal clear cell carcinoma. *J Immunol Res* 2022; 2022: 2818777.
- [76] Yu W, Wang G, Lu C, Liu C, Jiang L, Jiang Z, Liang Z, Wang X, Qin Z and Yan J. Pharmacological mechanism of Shenlingbaizhu formula against experimental colitis. *Phytomedicine* 2022; 98: 153961.
- [77] Ma C, Shi X, Guo W, Niu J and Wang G. miR-107 enhances the sensitivity of breast cancer cells to paclitaxel. *Open Med (Wars)* 2019; 14: 456-466.
- [78] Zhong Z, Lv M and Chen J. Screening differential circular RNA expression profiles reveals the regulatory role of circTCF25-miR-103a-3p/miR-107-CDK6 pathway in bladder carcinoma. *Sci Rep* 2016; 6: 30919.
- [79] Chen L, Li ZY, Xu SY, Zhang XJ, Zhang Y, Luo K and Li WP. Upregulation of miR-107 inhibits glioma angiogenesis and VEGF expression. *Cell Mol Neurobiol* 2016; 36: 113-120.
- [80] Chang Z, Fu Y, Jia Y, Gao M, Song L, Zhang W, Zhao R and Qin Y. Circ-SFMBT2 drives the malignant phenotypes of esophageal cancer by the miR-107-dependent regulation of SLC1A5. *Cancer Cell Int* 2021; 21: 495.

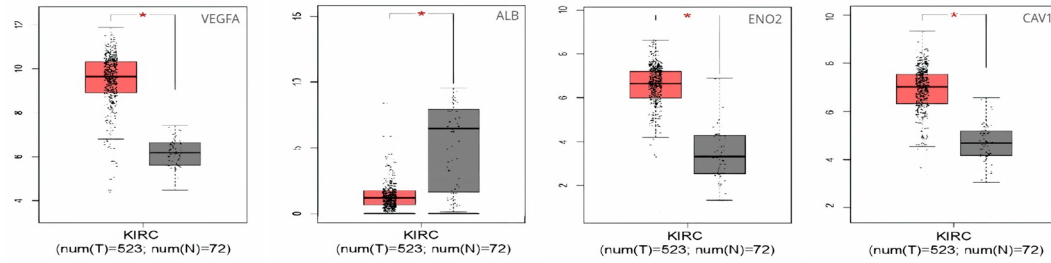
KIRC biomarkers



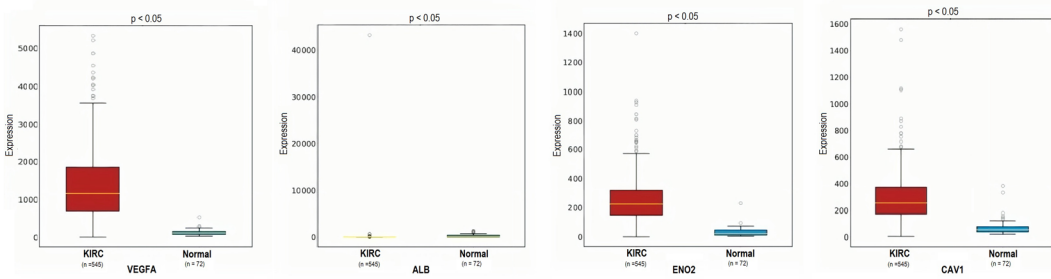
Supplementary Figure 1. Expression profiling of VEGFA, ALB, ENO2, and CAV1 in KIRC samples of different clinical variables relative to controls via UALCAN. (A) Expression profiling of VEGFA in KIRC samples of different clinical variables, (B) Expression profiling of ALB in KIRC samples of different clinical variables, (C) Expression profiling of ENO2 in KIRC samples of different clinical variables, and (D) Expression profiling of CAV1 in KIRC samples of different clinical variables.

KIRC biomarkers

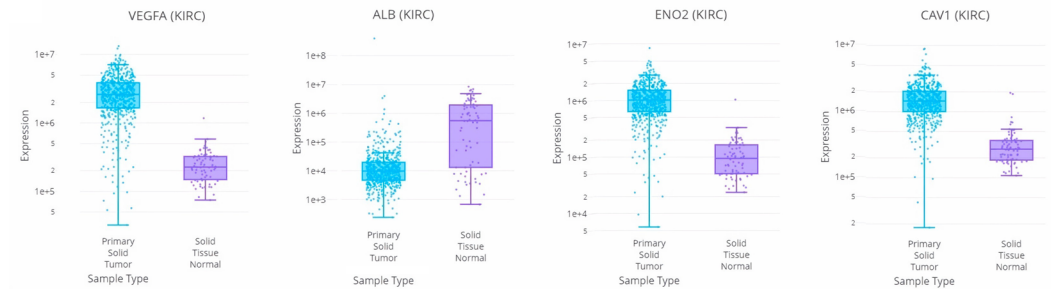
A



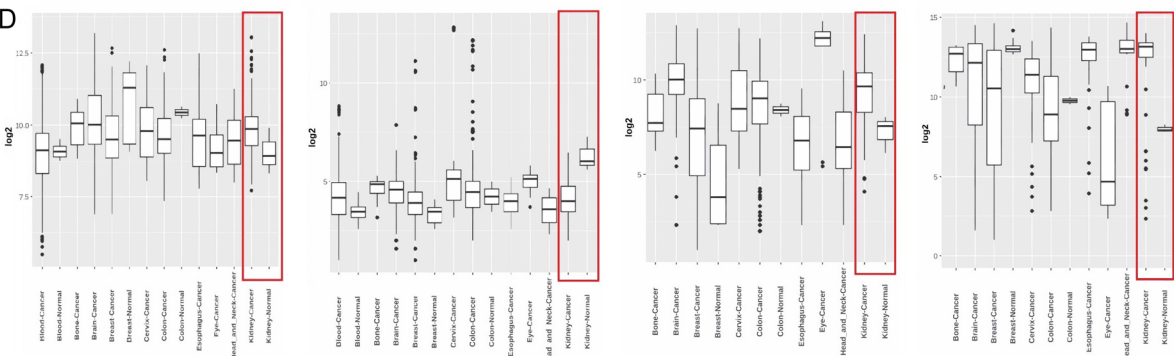
B



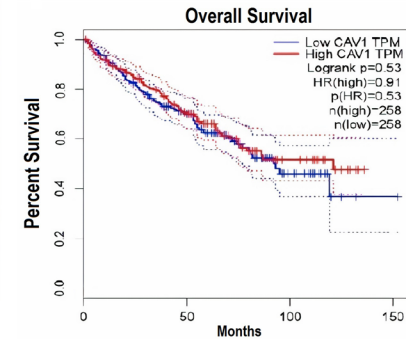
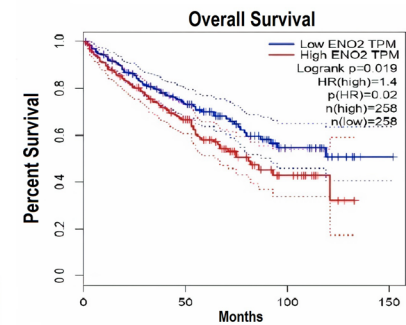
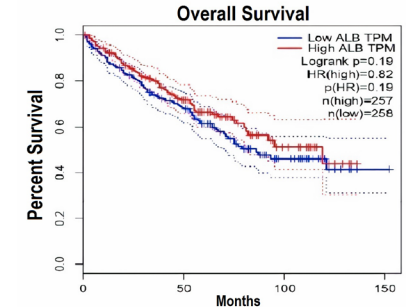
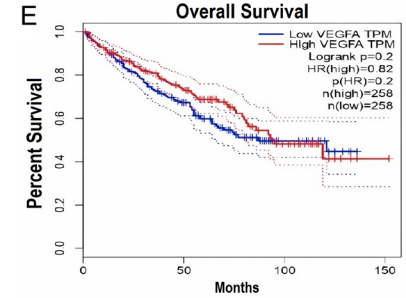
C



D

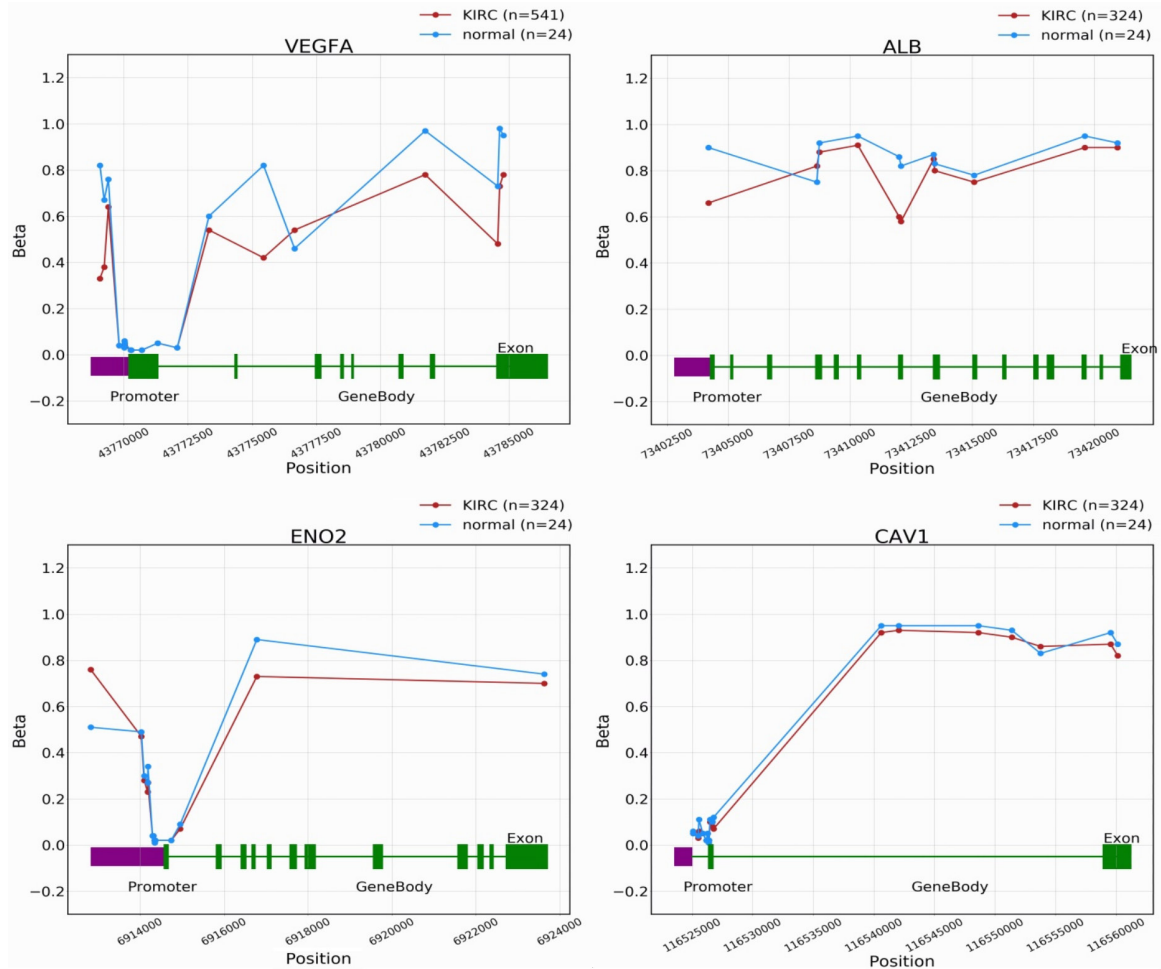


E



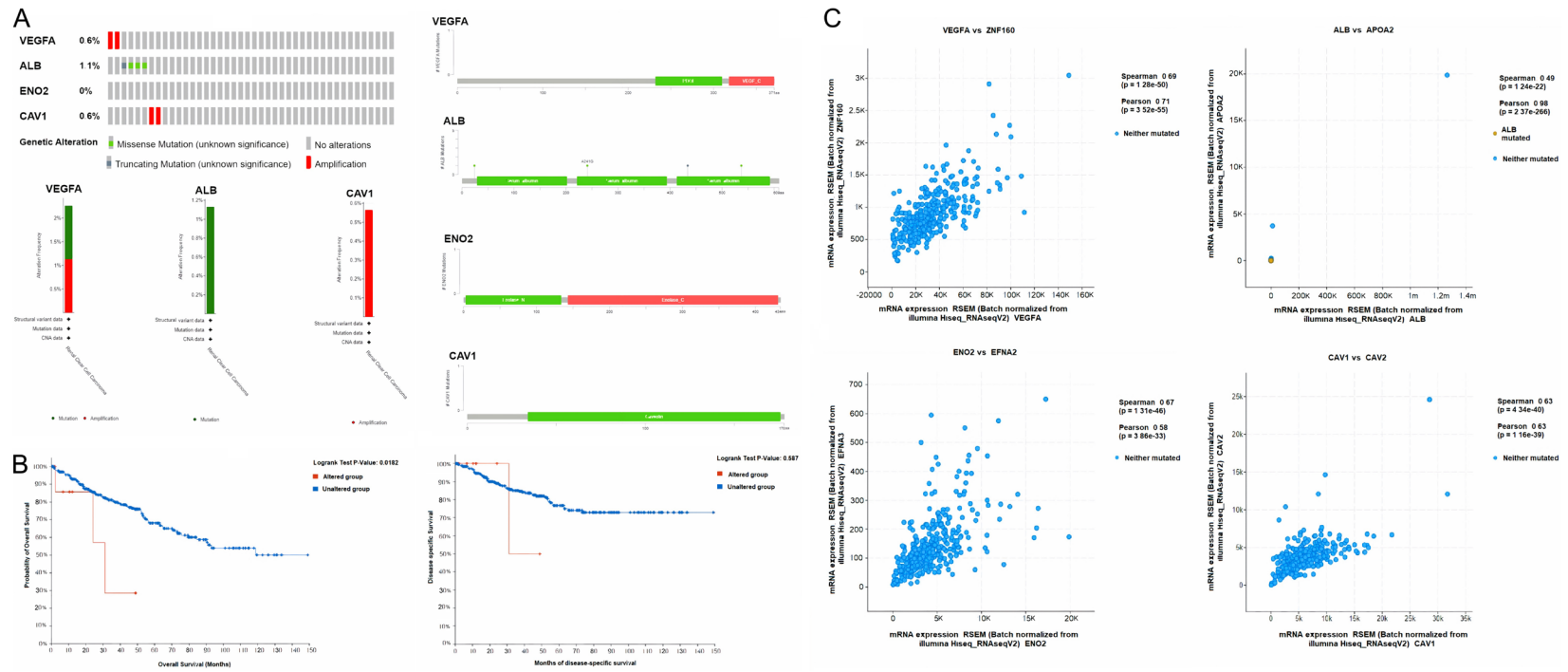
KIRC biomarkers

Supplementary Figure 2. Expression validation and survival analysis of VEGFA, ALB, ENO2, and CAV1. (A) Expression validation of VEGFA, ALB, ENO2, and CAV1 via GEPIA database, (B) Expression validation of VEGFA, ALB, ENO2, and CAV1 via OncoDB database, (C) Expression validation of VEGFA, ALB, ENO2, and CAV1 via DriverDBv3 database, (D) Expression validation of VEGFA, ALB, ENO2, and CAV1 via GENT2 database, and (E) Survival analysis of VEGFA, ALB, ENO2, and CAV1 via GEPIA database. *P < 0.05.



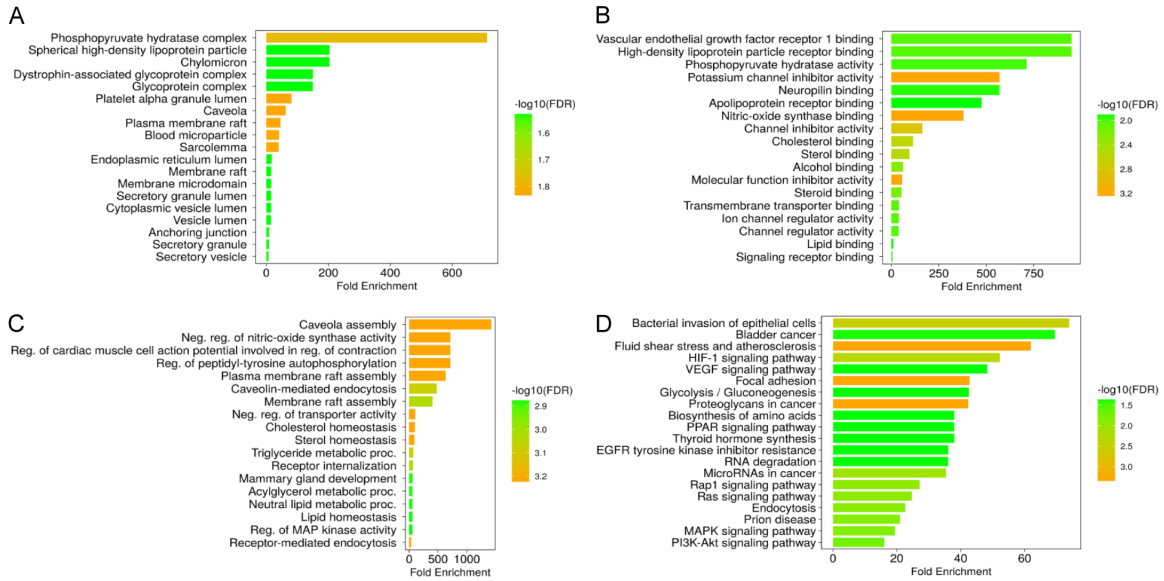
Supplementary Figure 3. Methylation status exploration of VEGFA, ALB, ENO2, and CAV1 via OncoDB in KIRC and normal samples.

KIRC biomarkers

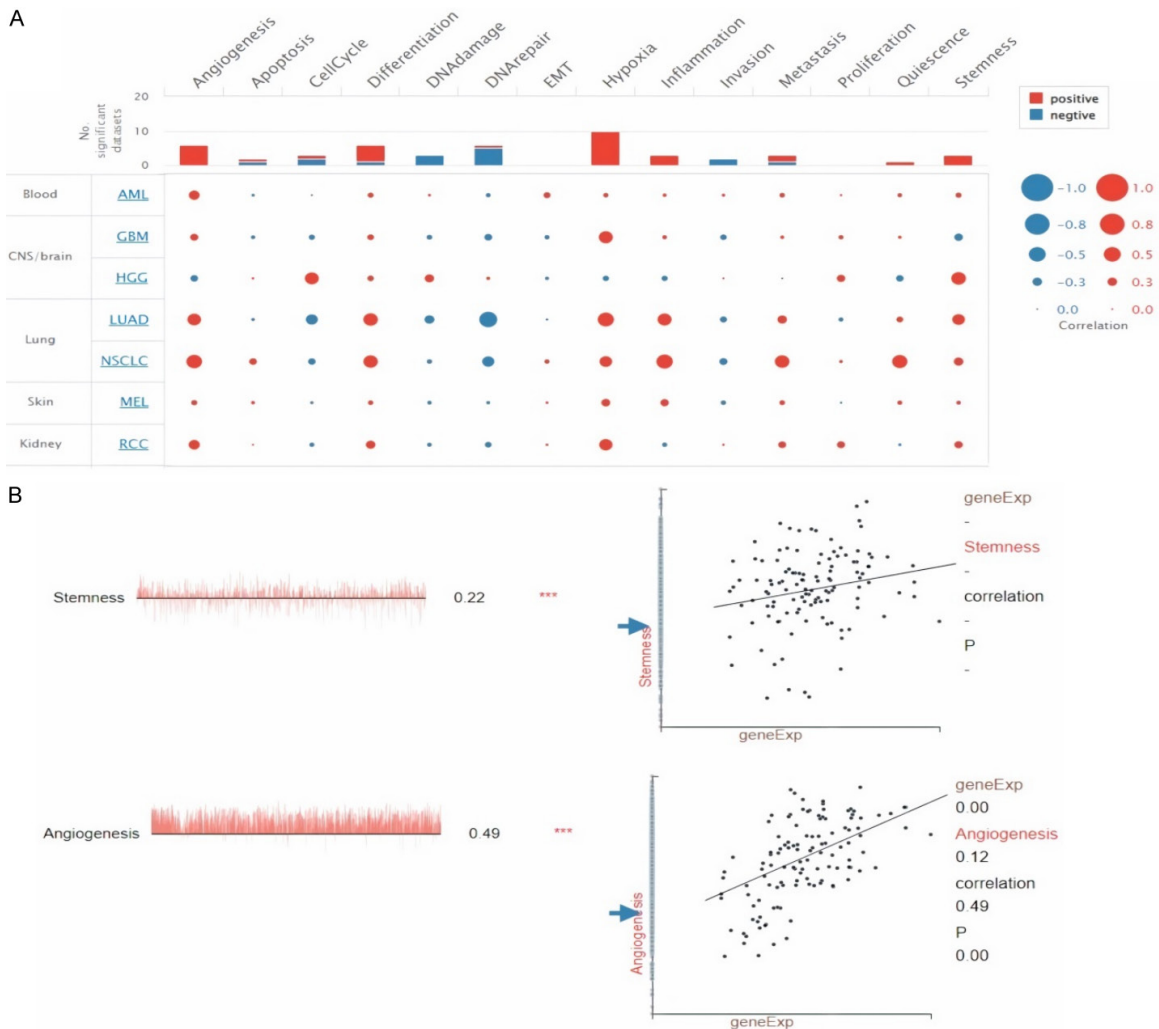


Supplementary Figure 4. Exploration of genetic alteration frequencies, mutational hotspots, OS, DFS analyses, and co-expressed genes of VEGFA, ALB, ENO2, and CAV1 in KIRC via cBioPortal. (A) Types, frequencies, and location of the genetic alterations in VEGFA, ALB, ENO2, and CAV1, (B) OS and DFS analysis of VEGFA, ALB, ENO2, and CAV1 in genetically altered and unaltered KIRC group, and (C) Identification of co-expressed genes with VEGFA, ALB, ENO2, and CAV1 in KIRC samples.

KIRC biomarkers

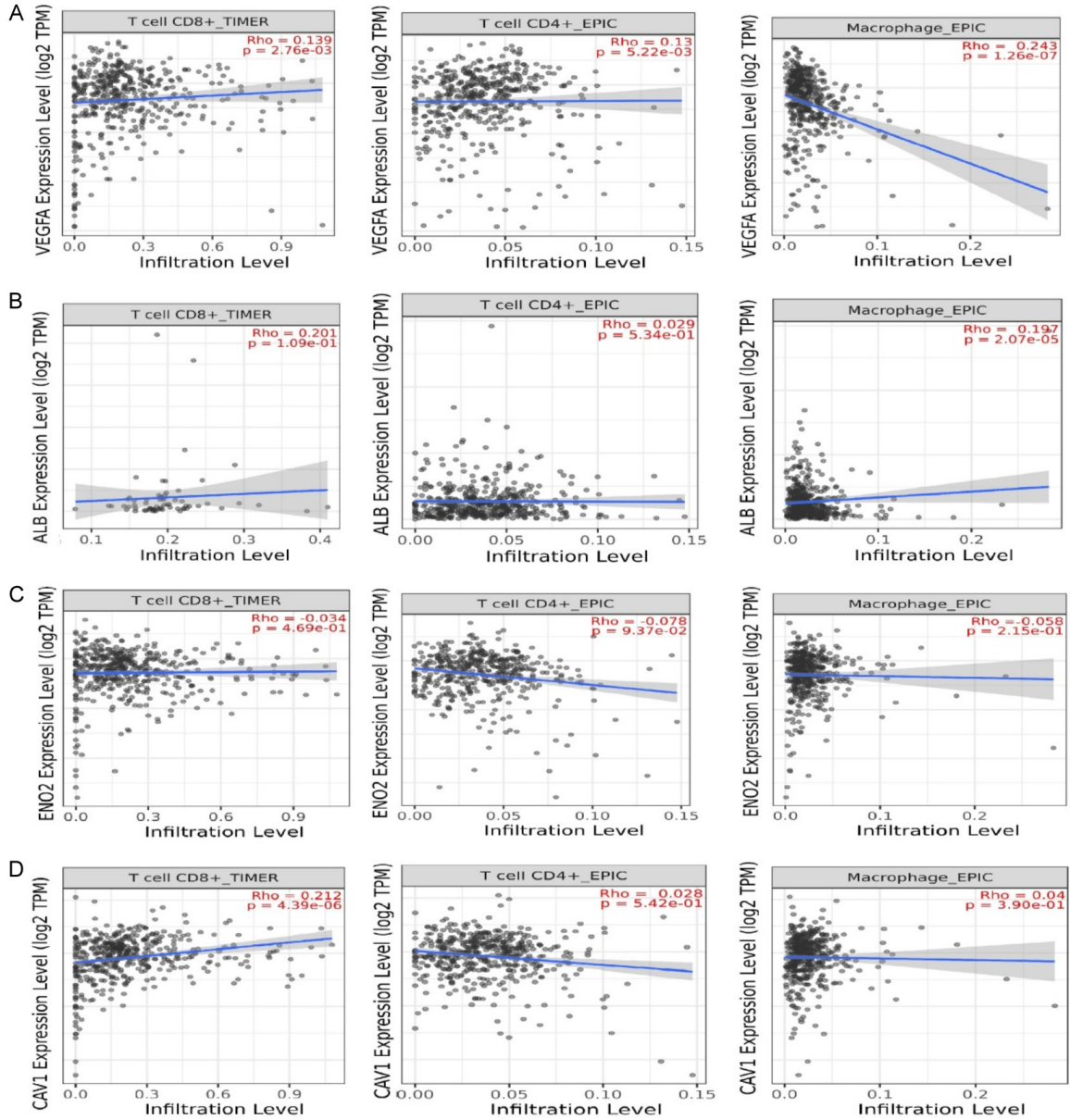


Supplementary Figure 5. Gene enrichment analysis of VEGFA, ALB, ENO2, and CAV1. (A) VEGFA, ALB, ENO2, and CAV1 associated CC terms, (B) VEGFA, ALB, ENO2, and CAV1 associated BP terms, (C) VEGFA, ALB, ENO2, and CAV1 associated MF terms, and (D) VEGFA, ALB, ENO2, and CAV1 associated KEGG terms.



KIRC biomarkers

Supplementary Figure 6. Association of VEGFA, ALB, ENO2, and CAV1 hub genes expression with fourteen different states in KIRC. (A) Overall associations (significant/insignificant) of VEGFA, ALB, ENO2, and CAV1 with angiogenesis, apoptosis, cell cycle and many others, and (B) Significant associations of VEGFA, ALB, ENO2, and CAV1 with stemness and angiogenesis.



Supplementary Figure 7. Correlation analysis of VEGFA, ALB, ENO2, and CAV1 hub genes expression with different immune cells (CD8+ T, CD4+ T, and Macrophages) infiltration level. (A) VEGFA, (B) ALB, (C) ENO2, and (D) CAV1.

KIRC biomarkers

